Journal of Molecular Structure 1132 (2017) 149–156

Contents lists available at ScienceDirect

Journal of Molecular Structure

journal homepage: http://www.elsevier.com/locate/molstruc

# Conformational properties of 1-cyano-1-silacyclohexane, $C_5H_{10}SiHCN$: Gas electron diffraction, low-temperature NMR and quantum chemical calculations☆

Alexander V. Belyakov [a], Yrii F. Sigolaev [a], Sergey A. Shlykov [b], Sunna Ó. Wallevik [c, 1], Nanna R. Jonsdottir [c], Sigridur Jonsdottir [c], Ágúst Kvaran [c], Ragnar Bjornsson [c], Ingvar Arnason [c, *]

[a] Saint-Petersburg State Technological Institute, Saint-Petersburg 190013, Russia
[b] Ivanovo State University of Chemistry and Technology, Sheremetev ave. 7, 153000, Ivanovo, Russia
[c] Science Institute, University of Iceland, Dunhaga 3, IS-107 Reykjavik, Iceland

ARTICLE INFO

*Article history:*
Received 7 July 2016
Received in revised form
23 September 2016
Accepted 4 October 2016
Available online 5 October 2016

*Keywords:*
Silacyclohexane
Molecular structure
Gas electron diffraction
Dynamic NMR spectroscopy
Quantum chemical calculations
Conformational analysis

ABSTRACT

The conformational preference of the cyano group of the 1-cyano-1-silacyclohexane was studied experimentally by means of gas electron diffraction (GED) and dynamic nuclear magnetic resonance (DNMR) as well as by quantum chemical (QC) calculations applying high-level coupled cluster methods as well as DFT methods. According to the GED experiment, the compound exists in the gas-phase as a mixture of two conformers possessing the chair conformation of the six-membered ring and $C_s$ symmetry while differing in the axial or equatorial position of the substituent (axial = 84(12) mol %/equatorial = 16(12) mol %) at $T = 279(3)$ K, corresponding to an $A$ value ($G_{ax} - G_{eq}$) of $-1.0(4)$ kcal mol$^{-1}$. Gas-phase CCSD(T) calculations predict an $A$ value of $-0.72$ kcal mol$^{-1}$ at 279 K. In contrast, the low-temperature $^{13}$C NMR experiments resulted in an axial/equatorial ratio of 35/65 mol % at 120 K corresponding to an $A$ value of 0.14 kcal mol$^{-1}$. An average value for $\Delta G^{\#}_{e\rightarrow a} = 5.6 \pm 0.1$ kcal mol$^{-1}$ was obtained for the temperature range 110–145 K. The dramatically different conformational behaviour in the gas-phase (GED) compared to the liquid phase (DNMR) suggests a strong solvation effect. According to natural bond orbital analysis the axial conformer of the title compound is an example of stabilization of a form, which is not favored by electrostatic effects and is favored predominantly by steric and conjugation effects.

## 1. Introduction

The stereochemistry of cyclohexane **1** is among the best explored areas in organic stereochemistry [1,2]. The chair-to-chair inversion in cyclohexane is well understood, the Gibbs free energy of activation for the step chair → half-chair$^{\#}$ → twist → half-chair$^{\#}$ → inverted chair is generally accepted to be 10.1–10.5 kcal mol$^{-1}$. Far fewer investigations have been reported on silicon-containing six-membered rings. In silacyclohexane **3** the activation energy is about one-half of the value for cyclohexane [3]. The conformational equilibrium of a large number of monosubstituted cyclohexanes has been studied. Winstein and Holness defined the *A*-value as the thermodynamic preference for the equatorial conformation over the axial one (see Scheme 1 for definition of *A*) [2,4]. A positive *A* value corresponds to a preference for the equatorial conformer and $\Delta G = G_{ax} - G_{eq} > 0$. All energy differences herein will be presented as (axial − equatorial). As a rule, in monosubstituted cyclohexanes, the substituent prefers the equatorial position of the chair conformation. Rare exceptions are substituents having mercury bonded to the cyclohexane ring [2]. When the substituent becomes bulkier its equatorial preference generally increases. The simplest alkyl groups; methyl, ethyl, isopropyl, and *t*-butyl have been used as examples. This tendency has in a classical way been ascribed to a 1,3-*syn*-diaxial interaction between the substituent in axial position and axial hydrogens on the ring carbon atoms in positions 3 and 5 [5]. Towards the end of

---

☆ In honour of Professor Georgiy Girichev on the occasion of his 70th birthday.
* Corresponding author.
*E-mail address:* ingvara@hi.is (I. Arnason).
[1] Present address: Rheocenter, Reykjavik University, IS-112 Reykjavik, Iceland.

http://dx.doi.org/10.1016/j.molstruc.2016.10.012

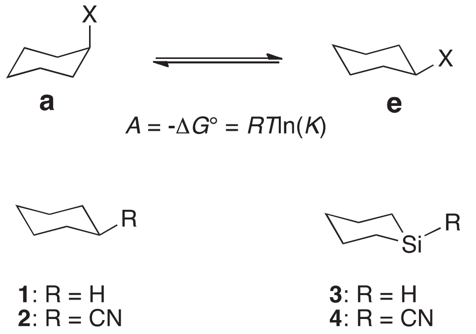

**Scheme 1.** Definition of the *A* value and structures of compounds **1** to **4**.

the last century, accepted *A* values were 1.74, 1.79, 2.21, and 4.9 kcal mol$^{-1}$ for Me, Et, *i*-Pr, and *t*-Bu, respectively [5–7]. Evidence that question the model of 1,3-*syn*-diaxial interaction is starting to appear. Wiberg et al. revised the *A* values for the three lightest alkyl groups and reported the values of 1.80, 1.75, and 1.96 kcal mol$^{-1}$ for Me, Et, and *i*-Pr respectively (all values reported with the error limit of $\pm$0.02 kcal mol$^{-1}$) and the authors concluded that there was no evidence of a 1,3-*syn*-diaxial interaction with the axial hydrogens at C(3,5) [8]. Taddei and Kleinpeter have examined the role of hyperconjugation in substituted cyclohexanes [9,10]. Cuevas et al. using atoms in molecules (AIM) analysis concluded that the *t*-Bu group is more stable when it adopts the axial position in cyclohexane but produces destabilization of the cyclohexyl ring [11]. Clearly the conformational preferences in monosubstituted cyclohexanes are still not fully understood. In recent years *A* values for some monosubstituted derivatives of **3** have been reported. Methyl [12–14], phenyl [15], and *t*-Bu [16] substituents were found to have positive *A* values, albeit much lower in magnitude than the corresponding cyclohexane analogues [17,18]. Other substituents like $CF_3$[19,20] and $SiH_3$[21] were found to prefer the axial position contrary to their cyclohexane analogues. The halogens are substituents of special interest being monoatomic with decreasing electronegativity and increasing size and polarizability as one goes down the halogen group. The *A* values of the halocyclohexanes have been reported a number of times using different methods [2,22]. In a recent study we reported on experimental and theoretical conformational properties of 1-halogenated-1-silacyclohexanes [23]. The calculated conformational energies Δ*E* (at CCSD(T)/CBS level of theory) are shown in Fig. 1. The calculated data are in good agreement with experimental results. The calculations were extended to include the halocyclohexanes and At derivatives as well.

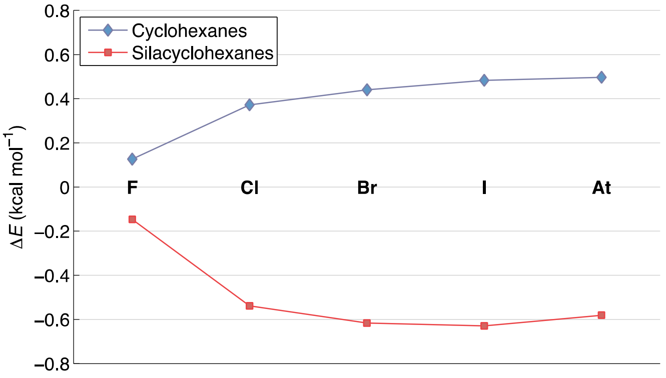

**Fig. 1.** Conformational energies $\Delta E = E_{ax} - E_{eq}$ for $C_6H_{11}X$ and $C_5H_{10}SiHX$ [23]. Copyright by the ACS Publications. Reproduced with permission.

It is remarkable to see the opposite behaviour of the two series. All halocyclohexanes show preference for the equatorial position whereas all silacyclohexanes show preference for the axial position of the halogen. Within each series the energy difference is lowest for the fluoro derivative but considerably higher for the heavier halogens. The cyanide ion is well known to exhibit pseudohalogenic character in main group chemistry [24]. It is therefore interesting to explore how cyanide as a substituent will fit into the results summarized in Fig. 1.

NMR conformational analysis of cyanocyclohexane **2** applying various methods using variable solvents at different temperatures have over the time consistently predicted positive *A* values in the range of 0.12–0.25 kcal mol$^{-1}$ [6,25–30]. Recently Durig et al. published a microwave (MW), Raman, and infrared (IR) spectroscopic study on **2** [31]. From IR spectra in xenon solution the axial conformer was found to be more stable by 0.18 $\pm$ 0.03 kcal mol$^{-1}$ ($\Delta H = -$ 0.18 $\pm$ 0.03 kcal mol$^{-1}$). The Raman effect of the liquid sample resulted in a similar value of 0.13 $\pm$ 0.05 kcal mol$^{-1}$ ($\Delta H = -$0.13 $\pm$ 0.05 kcal mol$^{-1}$). MP2(full)/6-311 + G(d,p) *ab initio* calculations predicted the axial form to be more stable by 0.34 kcal mol$^{-1}$ ($A = -$0.34 kcal mol$^{-1}$), whereas the B3LYP method with the same basis sets predicted the equatorial form to be more stable by 0.51 kcal mol$^{-1}$($A$ = +0.51 kcal mol$^{-1}$) [31].

The differences between cyclohexanes and silacyclohanes were recently discussed by Shainyan and Kleinpeter in a paper entitled “Silacyclohexanes and silaheterocyclo¬hexanes: why are they so different from other heterocyclohexanes?” One major conclusion made by the authors is that strong electrostatic and hyperconjugative effects of Si–C and Si–Hal bonds dominate the conformational equilibria of the corresponding silacyclohexanes [32].

In this paper, we report the first synthesis of the title compound **4** and conformational analysis of **4** using gas electron diffraction (GED) and dynamic NMR (DNMR) experiments as well as quantum chemical (QC) calculations of both **2** and **4** and compare the conformational properties of the cyanide group in silacyclohexane and cyclohexane.

## 2. Results

### 2.1. Gas electron diffraction

The structure optimizations of the axial and equatorial conformers of molecule **4** were carried out under $C_s$ symmetry. To reduce the number of refined parameters the following assumptions were made on the basis of M06-2X [33]/aug-cc-pVTZ results. Only the geometric parameters of the axial conformer were refined and the parameters of the equatorial form were tied to those of the axial conformer using the calculated differences. A molecular model and the atom numbering are shown in Fig. 2. For the axial conformer the difference between the nearly equal C2–C3 and C3–C4 bond lengths was constrained to the calculated value. All C–H bonds, H–C–H angles, and $H_{ax}$–C2–C3, $H_{eq}$–C3–C2, $H_{eq}$–C3–C4, and $H_{ax}$–C3–C2 angles are set equal. Angles that define the orientation of the C–H bonds were set to calculated values. Mean vibrational amplitudes of atom pairs were refined in five groups corresponding to the peaks of the radial distribution curve. The experimental and theoretical *f*(*r*) curves along with their differences Δ*f*(*r*) are given in Fig. 3. The final set of structural and vibrational parameter for the axial conformer is listed in Tables 1 and 2. According to the GED data, the axial conformer of **4** has an 84(12) mol % abundance in the vapor of **4** at 279(3) K. This value corresponds to an *A* value of −1.0(4) kcal mol$^{-1}$ (Table 1). As can be seen from Table 1, this result is in excellent agreement with DFT calculations using the M06-2X functional. Likewise, the molecular

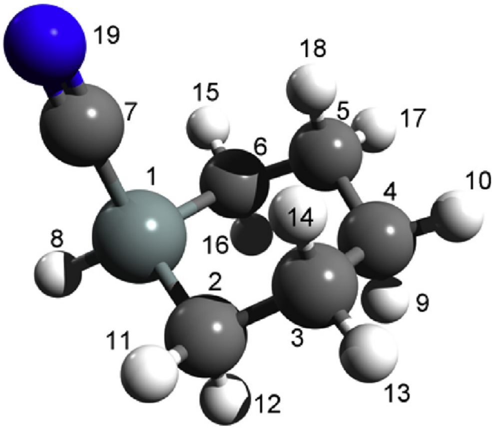

**Fig. 2.** Molecular model and atom numbering of 1-cyano-1-silacyclohexane **4** (axial conformer).

**Table 1**
Main geometrical parameters of the axial conformer of 1-cyano-1-silacyclohexane (**4**) molecular model of $C_s$ symmetry.[a]

| | M06-2X | GED |
|---|---|---|
| Δ *E* (kcal $mol^{-1}$) | 1.0 | |
| Δ *H*° $_{298}$ (kcal $mol^{-1}$) | 1.0 | |
| Δ *G*° $_{298}$ (kcal $mol^{-1}$) | 0.9 | 1.0(4) |
| $\chi_{ax}$ % | 82 | 84(12) |
| Bond lengths (in Å) | $r_e$ | $r_a$ |
| Si–C7 (*p1*) | 1.876 | 1.875(2) |
| Si–C2 *p1* | 1.867 | 1.866(2) |
| C2–C3 *p2* | 1.539 | 1.541(3) |
| C3–C4 (*p2*) | 1.531 | 1.533(3) |
| $(C–H)_{av}$ *p3* | 1.090 | 1.083(4) |
| Si–H *p4* | 1.475 | 1.475[b] |
| CN *p5* | 1.149 | 1.161(5) |
| Bond angles (in °)[c] | $\angle_e$ | $\angle_{h1}$ |
| C2–Si–C6 *p6* | 106.3 | 108.2(1.3) |
| C3–C4–C5*p7* | 114.2 | 113.5(1.6) |
| $(H–C–H)_{av}$ *p8* | 106.7 | 106.7[b] |
| C2–C3–C4[d] | 113.4 | 114.8(0.9) |
| Si–C2–C3[d] | 109.4 | 110.5(0.5) |
| C7–Si–C2[d] | 106.5 | 106.8(1.4) |
| C2–Si–C6–C5[d] | −44.8 | −37.9(3.9) |
| Si–C6–C5–C4[d] | 55.4 | 51.8(1.7) |
| C6–C5–C4–C3[d] | −66.4 | −66.1(1.5) |

Notes:
[a] Relative electronic energies at 0 K (Δ*E*); relative standard enthalpy (Δ*H*°), relative standard free energy (−Δ*G*°) and mole fraction (χ) in the gas-phase at 298 K at the M06-2X/aug-cc-pVTZ level of theory. *pi*–independent parameter, (*pi*)–difference equals theoretical one.
[b] Fixed.
[c] $H_{ax}$–C2–C3 = $H_{eq}$–C3–C2 = $H_{eq}$–C3–C4 = $H_{ax}$–C3–C2. *R-factor* = 4.9% was calculated using Eq. (1) in the experimental section; Parenthesized values are 3σ.
[d] Dependent.

structure derived from the GED experiment is very well predicted by the M06-2X calculations. (Table 1).

### 2.2. Dynamic NMR spectroscopy (DNMR)

The $^{13}$C NMR spectra of **4** were recorded in the temperature range from 110 to 160 K. At 160 K the spectra are in agreement with a rapid interconversion of the two chair forms. On cooling below 140 K the spectra show a large line broadening and gradual splitting of signals into a main signal and a smaller one, indicating a mixture of a major and a minor conformer. This effect, which is most pronounced for the C3 and C5 atoms (around 24 ppm), is shown in Fig. 4. As a general rule in cyclohexane chemistry, the resonance signals of the axial conformer are shifted to lower δ values [34–37] and the same has been found to be true for the substituted silacyclohexanes [12,15,21,23]. QC calculations of the chemical shifts may be used to further confirm assignments of signals to the conformations in question. Table 3 shows the calculated chemical (and experimental) shifts for the ring carbon atoms in **4**. The carbon atoms C3 and C5 are predicted to have 0.90 ppm higher chemical shift in the equatorial conformer than in the axial one. The experimental difference is 0.91 ppm at 110 K (Fig. 4). Therefore, the major component is assigned to the equatorial conformer.

Based on this signal assignment, dynamic NMR simulations of the C3(5) signals using the software WinDNMR [38] as shown in Fig. 5 allowed determination of the rate constants ($k_{e\to a}$) and the corresponding free energies of activation ($\Delta G^{\#}_{e\to a}$) as a function of temperature. Chemical shifts, derived from NMR spectra, which were recorded at the lowest temperatures, were assumed to represent conditions of negligible interconversions. An average value for $\Delta G^{\#}_{e\to a} = 5.6 \pm 0.1$ kcal $mol^{-1}$ was obtained for the temperature range 110–145 K. Furthermore, the equilibrium constant ($K_{e\to a}$) and the free energy difference ($\Delta G_{e\to a}$), for the equatorial to axial transformations, corresponding to 120 K (a temperature close to the coalescence point) were determined from the relative signal intensities ($K_{e\to a}$ = 0.55 and

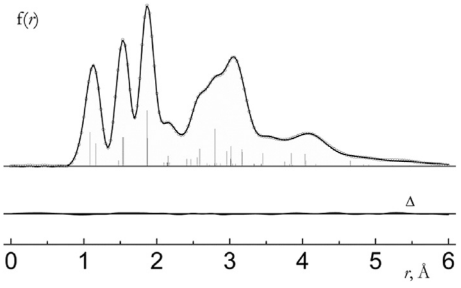

**Fig. 3.** Experimental (dots) and calculated (solid lines) radial distribution curve for the axial conformer of 1-cyano-1-silacyclohexane **4** as obtained by gas electron diffraction. Below: difference curve (experiment − model).

**Table 2**
Experimental structural parameters (GED) of the axial conformer of 1-cyano-1-silacyclohexane molecule (**4**) (bond lengths $r_a$ in Å, bond angles $\angle h_1$ in °, amplitudes *u* in Å, and vibrational corrections $r_{h1} - r_a$ in $10^{-4}$ Å) and M06-2X/aug-cc-pVTZ values for geometric and vibrational parameters.

| Parameters | GED | | M06-2X | | |
|---|---|---|---|---|---|
| | $r_a$ | *u* | $r_e$ | *u* | $r_{h1}-r_a$ |
| Si–C2 | 1.866(2) | 0.052(2) | 1.867 | 0.051 | 6 |
| Si–C7 | 1.875(2) | 0.053(2) | 1.876 | 0.051 | 3 |
| C2–C3 | 1.541(3) | 0.054(2) | 1.539 | 0.052 | 9 |
| C3–C4 | 1.533(3) | 0.052(2) | 1.531 | 0.051 | 6 |
| C≡N | 1.161(5) | 0.035(5) | 1.149 | 0.033 | 7 |
| $C–H_{av}$ | 1.083 (4) | 0.078(5) | 1.090 | 0.076 | 17 |
| Si–H | $1.475_{fixed}$ | 0.089(2) | 1.475 | 0.087 | 17 |
| C7⋯C2 | 2.998(26) | 0.107(5) | 2.999 | 0.095 | 67 |
| C7⋯C3 | 3.565(64) | 0.209(22) | 3.451 | 0.185 | 168 |
| C7⋯C4 | 4.157(77) | 0.213(22) | 4.032 | 0.189 | 212 |
| Si⋯C3 | 2.802(8) | 0.082(5) | 2.786 | 0.070 | 54 |
| Si⋯C4 | 3.162(20) | 0.089(5) | 3.152 | 0.077 | 82 |
| Si⋯N | 3.030(5) | 0.067(5) | 3.024 | 0.055 | 70 |
| C2⋯C4 | 2.588(13) | 0.079(5) | 2.567 | 0.067 | 37 |
| C3⋯C5 | 2.560(23) | 0.081(5) | 2.572 | 0.069 | 47 |
| C2⋯C6 | 3.020(25) | 0.097(5) | 2.988 | 0.084 | 45 |
| C2⋯C5 | 3.178(12) | 0.088(5) | 3.171 | 0.076 | 57 |
| C2⋯N | 4.046(30) | 0.180(22) | 3.968 | 0.156 | −478 |
| C3⋯N | 4.527(80) | 0.331(22) | 4.205 | 0.307 | −1192 |
| C4⋯N | 5.182(97) | 0.347(24) | 4.827 | 0.323 | −1251 |

Note: Parenthesized values are 3σ.

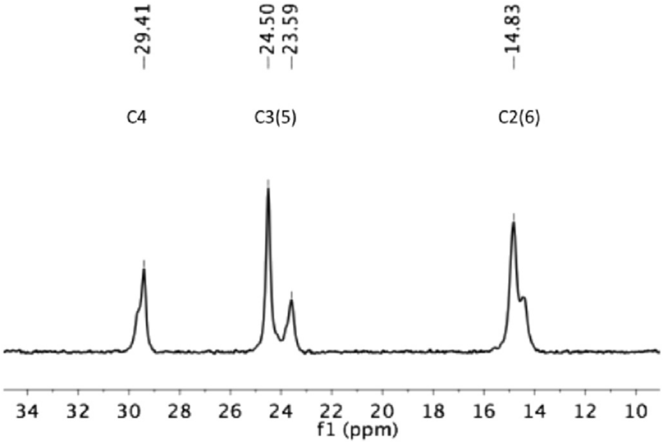

**Fig. 4.** $^{13}$C NMR spectrum of 1-cyano-1-sila-cyclohexane **4** at 110 K.

$\Delta G_{e\rightarrow a} = 0.14$ kcal mol$^{-1}$). This corresponds to about 65/35 mol % mixture of the equatorial and axial conformers.

### 2.3. Quantum chemical calculations

In the present work the partitioning of the total electronic energy $E^{(tot)}$ into Lewis $E^{(L)}$ (orbital population $n_i = 2.0$) and non-Lewis $E^{(NL)}$ parts (see Table 4) is performed using the concept of natural bond orbital (NBO) analysis. The localized Lewis component $E^{(L)}$ corresponds to more than 99.5% of the full electron density, and incorporates in good approximation all steric and classic electrostatic effects. The non-Lewis $E^{(NL)}$ part describes all types of conjugation. Table 4 shows that if only effects of conjugations would be considered, the axial conformation of **4** would be more preferable. The total steric energy $E^{(ST)}$ from the NBO analysis was calculated as described in Refs. [39–41] The Natural Coulomb Electrostatic energies $E^{(NCE)}$, total and its Lewis components, were calculated as described in [42]. Table 4 further shows that steric interactions in the axial conformer are more pronounced than in the equatorial conformer. It is to be noted that from the point of view of total steric energy at the HF/6-311++G** level of theory, the axial conformer of **4** is on the contrary more stable by 2.8 kcal mol$^{-1}$. This may be attributed to the details of parameterizations of DFT methods as compared with the HF method and may lead to DFT methods being useless for evaluation of steric energy (see Ref. [42] p.123). Thus, as it follows from Table 4, the axial conformer of molecule **4** is an example of stabilization of a form, which is not favored by electrostatic effects and is favored predominantly by steric and conjugation effects. For molecule **2** the non-Lewis part of the total energy ($E^{(NL)}$), that is conjugations, plays an important role in stabilization of the equatorial conformer (see Table 4).

Explicitly correlated [43] MP2 and coupled cluster calculations were carried out in order to derive a CCSD(T)/CBS (complete basis set limit) estimated electronic energy difference between axial and equatorial conformers of both cyanocyclohexane (**2**) and silacyclohexane (**4**). The explicitly correlated methodology should ensure rapid basis set convergence while use of the CCSD(T) method (the gold standard of quantum chemistry) captures most of the important dynamic correlation energy (see computational details for more information). Shown in Table 5 are CCSD(T)/CBS calculated relative energies with DFT-computed zero-point energy (ZPE) and thermochemical corrections at experimental temperatures, compared to the experimental IR and Raman enthalpy differences of **2** [31] and the experimental GED (at 279 K) and low-temperature DNMR (at 120 K) free energy differences of **4**. The M06-2X value (−1.0 kcal mol$^{-1}$) is close to the CCSD(T) $\Delta E$ value (−0.79 kcal mol$^{-1}$).

**Table 3**
Calculated chemical shifts (relative to TMS, ppm) for the ring carbon atoms in the axial and equatorial conformers of 1-cyano-1-silacyclohexane (**4**). Experimental values at 110 K are shown in parentheses.

| C atom | Axial/calc. (exp.) | Equatorial/calc. (exp.) | Ax.−Eq./calc. (exp.) |
|---|---|---|---|
| 2(6) | 13.34 (*14.45*) | 13.57 (*14.83*) | −0.23 (*−0.38*) |
| 3(5) | 28.39 (*23.59*) | 29.29 (*24.50*) | −0.90 (*−0.91*) |
| 4 | 34.07 (*29.41*) | 33.78 (*29.62*) | 0.29 (*0.21*) |

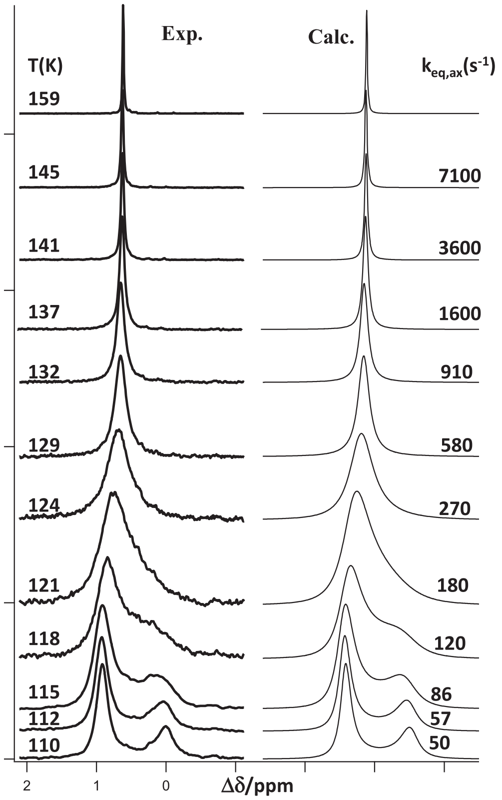

**Fig. 5.** Low-temperature $^{13}$C NMR spectra for the C3 and C5 atoms of **4**. Simulated spectra are shifted to the right of the experimental spectra for clarity reason.

**Table 4**
Results of the NBO analysis and energy decomposition of total electronic energy $E^{(total)}$ into Lewis $E^{(L)}$, non-Lewis $E^{(NL)}$, total steric $E^{(ST)}$ and electrostatic $E^{(NCE)}$ energies at the M06-2X/6-311++G** level of theory. Relative energies are in kcal mol$^{-1}$.

| NBO analysis | (CN) $SiH(CH_2CH_2)_2CH_2$ (4) | | (CN) $CH(CH_2CH_2)_2CH_2$ (2) | |
|---|---|---|---|---|
| | *ax* | *eq* | *ax* | *eq* |
| $\Delta E^{(tot)}$ | 0.0 | 1.0 | 0.0 | 0.4 |
| $\Delta E^{(L)}$ | 1.7 | 0.0 | 0.0 | 1.8 |
| $\Delta E^{(NL)}$ | 0.0 | 2.8 | 1.4 | 0.0 |
| $\Delta E^{(ST)a}$ | 10.4 | 0.0 | 0.3 | 0.0 |
| $\Delta E^{(NCE\text{-}tot)}$ | 3.9 | 0.0 | 0.0 | 1.2 |
| $\Delta E^{[NCE(L)]}$ | 3.3 | 0.0 | 0.0 | 1.6 |

Note:
[a] For the *axial* conformers of **4** and **2** at the HF/6-311++G** level of theory, $\Delta E^{(ST)}$ is −2.8 and −1.7 kcal mol$^{-1}$, respectively (see text).

**Table 5**
Conformational properties of cyanocyclohexane (**2**) and cyanosilacyclohexane (**4**). Computed Δ$E$ values are potential energy differences at 0 K (without ZPE or thermal contributions). Computed Δ$H$ values include ZPE and thermal contribution (at indicated temperature) and Δ$G$ values additionally include an entropic term.

| Method | $\Delta E = E_{ax} - E_{eq}$ (kcal mol$^{-1}$) | $\Delta H = H_{ax} - H_{eq}$ (kcal mol$^{-1}$) | $A = G_{ax} - G_{eq}$ (kcal mol$^{-1}$) |
|---|---|---|---|
| **(2)** | | | |
| CCSD(T)/CBS + therm.corr | −0.03 | +0.03 at 298 K | 0.16 at 298 K |
| *IR(Xenon)* | | −0.18 ± 0.03[a] | |
| *Raman(neat liq.)* | | −0.13 ± 0.05[a] | |
| *NMR* | | | 0.24 at 193 K[b] |
| **(4)** | | | |
| CCSD(T)/CBS + therm.corr | −0.79 | −0.79 | −0.72 at 279 K; −0.75 at 120 K |
| GED | | | −1.0 ± 0.4[c] |
| DNMR | | | +0.14[d] |

[a] From Ref. [31] Temperature range is 173–213 K for the IR exp. and 296–332 K for the Raman exp.
[b] From Ref. [27].
[c] This work. GED temperature is 279 K.
[d] This work. NMR temperature is 120 K.

## 3. Discussion

The GED results reveal a predominant axial preference for the silacyclohexane **4** in a very good agreement with (gas-phase) quantum chemical calculations, both M06-2X DFT and CCSD(T)/CBS calculations. The gas-phase axial preference of **4** is even more pronounced than that of 1-halo-1-silacyclohexanes (see Fig. 1) [23]. Surprisingly, the DNMR experiment at low temperatures in solution (a solvent mixture of $CD_2Cl_2$, $CHF_2Cl$, and $CF_3Br$) resulted in an equatorial preference and an axial/equatorial ratio of 35/65 mol % at 120 K. There is no doubt about the NMR signal splitting into one major and one minor components with cooling (Fig. 5). The signal assignments to axial and equatorial conformers are based on (i) a general rule found for other Si-monosubstituted silacyclohexanes that the C3 and C5 ring atom signals in the axial form are shifted to lower δ values compared to those in the equatorial form (Fig. 4) and (ii) the relative chemical shifts predicted by QC calculations (Table 3).

The equatorial preference at 120 K in the DNMR experiment is at odds with our best QC calculations as well as the GED result (see Table 5). It is still unclear what factors determine the stability of the equatorial conformer according to the DNMR experiment at 120 K in solution that may not be taken account of by the calculations. Whereas a solvation effect, possibly related to the polarity of the cyano group, we note that continuum solvation calculations, by using both the COSMO [44] and SMD [45] solvation models (implicit solvation models), were carried out separately at the B3LYP [46–49]-D3BJ [50,51]/def2-TZVP [52] level (using both an infinite dielectric constant and the dielectric constant of dichloromethane). Those calculations predicted, however, a shift of ~0.1 kcal mol$^{-1}$ towards further axial stabilization. Most likely a more explicit solvation effect is responsible for this differing conformational behaviour. Alternative possibility is a low-temperature entropy effect that is not described well using the harmonic approximation. In any event, the conformational properties of compound **4** appear to be very sensitive to the experimental conditions.

The present case of silacyclohexane **4** is the first example of a monosubstituted silacyclohexane compound of the general formula $C_5H_{10}SiHX$ that is found, by experiment, to have different conformational preferences in the gas-phase and in a solution. It should be noted that all monosubstituted silacyclohexanes that, hitherto, have been studied experimentally both in the gas-phase at approximate ambient temperatures (GED, MW) and in solutions at low temperatures (DNMR and temperature-dependent Raman experiments) have the same sign of the *A* value in both phases. Most substituents (F [53,54], Cl [23], Br [23], I [23,55], $CF_3$ [14,19,20], and $SiH_3$ [21]) give negative *A* values (axial preference) both in the gas-phase and in solutions. On the other hand Me [12–14] and Ph [15,56] substituents give positive *A* values both in gas-phase and in solutions. In this context, however, it is notable that some 1-methyl-3-hetero(X)-1-silacyclohexanes (X = NMe [57], O [58], and S [59,60]) also show Me-axial preferences in the gas-phase (GED) but Me-equatorial preferences by DNMR in solutions.

Let's now consider the cyclohexane counterpart **2** (cyanocyclohexane) and its conformational properties in comparison. For decades the only studies known were based on NMR analysis, which all consistently predicted an equatorial conformer preference (i.e. positive *A* values) in the range of 0.12–0.25 kcal mol$^{-1}$ [6,25–30]. Solvents like $CFCl_3$ [26,29], $CCl_4$ [28] and $CS_2$ [27] were applied in the NMR experiments. A recent combined FT-microwave, Raman and infrared spectroscopy study (IR in Xenon solution and Raman for neat liquid) by Durig et al. [31] on the other hand resulted in negative Δ$H$ values, (Table 5). QC calculations reported by Durig were as follows: MP2(full)/6-311 + G(d,p) *ab initio* calculations predicted the axial form to be more stable by 0.34 kcal mol$^{-1}$ whereas the B3LYP method with the same basis sets predicted the equatorial form to be more stable by 0.51 kcal mol$^{-1}$. Our CCSD(T)/CBS + thermal correction calculations, however, predict a gas-phase *A* value of 0.16 kcal mol$^{-1}$ in good agreement with the early NMR results as shown in Table 5, but we note that the *A* value changes sign when zero-point, thermal corrections and entropic effects are accounted for. The *A* value of **2** may of course also depend on solvent effects present in the NMR experiments. Clearly complications in terms of conformational preferences are also present in **2**.

Coming back to the question of whether the cyano group has pseudohalogen character, we now compare the *A* value of the cyano group with those for the halogen series (F, Cl, Br, I and At) for both the cyclohexane and silacyclohexane families. This comparison is best done by comparing calculated relative electronic energies at 0 K (Δ$E$) at the reliable CCSD(T)/CBS level, that are not dependent on environmental effects and experimental conditions (see Fig. 6).

Fig. 6 reveals that the cyano group exhibits a dramatically different properties in cyclohexane than in silacyclohexane. In cyclohexane, the energy difference of axial and equatorial is close to zero kcal mol$^{-1}$ and are closest to that found for the very electronegative fluorine substituent. In contrast, for the silacyclohexane family where the trends for the halogen substituents are very different, the cyano group has a strong axial preference, stronger than any halogen, but closest to the heavy bromine/iodine/astatine substituents.

## 4. Conclusions

The aim of this work was to explore the conformational properties of the cyano group as a 1-silacyclohexane substituent. A comparison with the 1-halo-1-silacyclohexanes as well as the

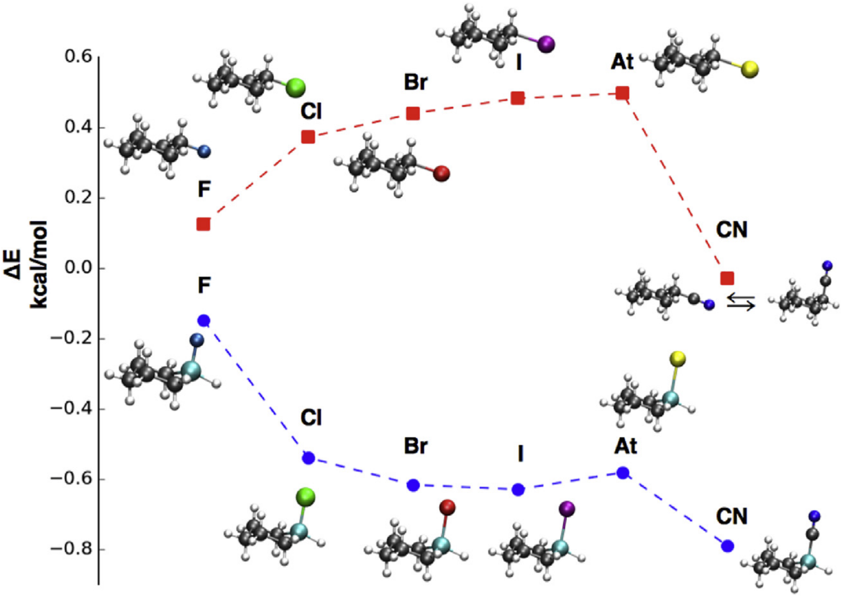

**Fig. 6.** CCSD(T)/CBS computed axial/equatorial energy differences (kcal $mol^{-1}$) of the halogen substituent series and the cyano group in both cyclohexane (red squares) and silacyclohexane families (blue circles). Also shown are the dominant conformers for each compound (cyano-cyclohexane energy difference is so close to zero that both conformers are shown). Lines are drawn to guide the eye. Modified from Fig. 1 and reproduced with permission [23]. (For interpretation of the references to colour in this figure legend, the reader is referred to the web version of this article.)

halogen- and cyano-substituted cyclohexanes was made. A close relationship between the effect of the cyano group (often claimed to be a pseudohalogen) and the halogens was not found. One might suspect the cyano group to behave like kind of a conformational chameleon. The cyano group might be expected to have different electronic properties whether bonded to Si or C but a dramatic different conformational behaviour observed for the cyclohexane and the silacyclohexane families, as seen in Fig. 6, is nonetheless striking. Perhaps the simplest way to account for this different behaviour may come from a comparison of the charge distribution in **2** and **4**. Whereas the carbon atom of the cyano substituent in **2** has a positive NBO charge (~+0.29 for both ax and eq) at the PBE0/def2-TZVPP level this changes to a negative partial charge (~−0.13 for both ax and eq), due to the bonding to the electropositive Si atom in **4**. Explaining why the conformational behaviour of the cyclohexane and silacyclohexane families are so different for equivalent substituents remains a challenging mystery, however.

In that respect, we strongly encourage further conformational studies of saturated six-membered heterocycles bearing a CN group at the heteroatom.

## 5. Experimental

### 5.1. Synthesis

Standard Schlenk techniques and an inert atmosphere of dry nitrogen were used for all manipulations. 1-Chloro-1-silacyclohexane was prepared as previously reported [23].

*1-Cyano-1-silacyclohexane***4**. Sodium cyanide (6.1 g, 123.9 mmol) was dried by continuous heating in vacuum for 24 h and was then added to a stirred mixture of zinc iodide (0.17 g, 0.5 mmol), polyethylene glycol (1.4 g) and 1-chloro-1-silacyclohexane (13.9 g, 103.2 mmol) dissolved in $CH_2Cl_2$ (35 mL). The reaction mixture was stirred for 24 h and then filtered under reduced pressure and the salt was discarded. The solvent was removed at reduced pressure and the desired product was collected by distillation at 152–153 °C and 1 atm (9.06 g, 72.3 mmol, 70%). $^1H$ NMR (400 MHz, $CDCl_3$): $\delta$ = 0.82–0.90 (m, 2H, $CH_{2(ax/eq)}$), 1.01–1.09 (m, 2H, $CH_{2(ax/eq)}$), 1.24–1.34 (m, 1H, $CH_{2(ax/eq)}$), 1.59–1.67 (m, 1H, $CH_{2(ax/eq)}$), 1.68–1.79 (m, 2H, $CH_{2(ax/eq)}$), 1.85–1.95 (m, 2H, $CH_{2(ax/eq)}$), 4.20–4.22 (m, $^1J_{H-Si}$ = 222 Hz, 1H, SiH). $^{13}C\{^1H\}$ NMR (101 MHz, $CDCl_3$: $\delta$ = 8.5, 23.6, 28.6, 124.1 (CN). $^{29}Si\{^1H\}$ NMR (79 MHz, $CDCl_3$): $\delta = -36.1$.

### 5.2. GED experiment

The combined gas electron diffraction and mass spectrometric experiment, GED/MS [61–63] was carried out at the stainless steel effusion cell temperature 279(3) K. The scattered electrons were collected on Kodak S0-163 EM films of 9 × 12 $cm^2$. Two camera distances, 598 (long) and 338 mm (short), were used, resulting in diffraction patterns in *s*-ranges of 2.0–17.2 $Å^{-1}$ and 5.6–30.6 $Å^{-1}$, respectively at *ca* 98 kV of accelerating voltage. The accurate electron wavelengths, 0.03757(4) Å and 0.03728(4) Å, for long and short distances, respectively, were measured from diffraction patterns of polycrystalline ZnO. The diffraction patterns of 1-cyano-1-silacyclohexane were recorded with (long/short) 0.6/1.0 μA primary electron beam intensities, 50/90 s exposure times, and a residual pressures of (2/3) x $10^{-6}$ Torr (GED unit) and (7/9) x $10^{-7}$ Torr (MS block). The optical densities of the diffraction patterns were measured by a computer controlled MD-100 (Carl Zeiss, Jena) microdensitometer [64]. The molecular scattering function, $sM(s)$, was evaluated as $sM(s) = (I_t(s)/I_b(s)-1)s$, where $I_t(s)$ is the total electron scattering intensity, $I_b(s)$ is the experimental background. After crossing the fast electrons beam in the diffraction chamber, the molecular beam from the effusion cell entered directly the ionization chamber of a monopole mass spectrometer attached to the GED unit. This allows real-time monitoring of the vapor composition by recording the mass spectra simultaneously with recording the diffraction patterns. Mass spectra recorded at ionizing voltage 50 V was represented by the parent ion ($m/z$ = 125 Da) and a set of daughter ions formed under electron impact. No peaks with the mass exceeding that of the molecular ion or caused by impurities, decomposition products, etc., were detected in the mass spectrum. In addition, the mass spectra at different ionizing voltages were measured, demonstrating the decrease of the daughter ions contribution as the ionizing electrons energy lowers.

When refining structural parameters the minimized functional has the form:

$$Q = \sum_s w_s \Delta_s^2 = \sum_s w_s \left[ s\,\mathrm{M}^{obs}(s) - k \cdot s\,\mathrm{M}^{cal}(s) \right]^2$$

where: $w_s$ is a weight function; $s = (4\pi/\lambda)\sin(\theta/2)$ is parameter of scattering angle $\theta$; $\lambda$ is wavelength of electron beam; $s\mathrm{M}(s)$ is the molecular intensity function and $k$ is the scale factor. As a criterion of minimum of the functional serves the value of $R$-factor:

$$R = \left( Q \Big/ \sum_s w_s \left( s\,\mathrm{M}^{obs}(s) \right)^2 \right)^{1/2} \quad (1)$$

The atomic scattering factors were taken from Ref. [65] Experimental backgrounds were drawn as cubic spline functions to the difference between experimental and theoretical molecular intensity curves using a program written by A. V. Belyakov.

Least-squares structure refinements were carried out with a modified version of the program KCED25 [66,67]. Weight matrices were diagonal. The short distance data were assigned the weight of 0.5 and the long distance data weights equal 1.0.

Estimated standard deviations calculated by the program were multiplied by a factor of three to include added uncertainty due to data correlation and an estimated scale uncertainty of 0.1%. The experimental and theoretical $s\mathrm{M}(s)$ curves along with their differences $\Delta s\mathrm{M}(s)$ are given in Fig. 7.

### 5.3. NMR experiment

A 400 MHz NMR spectrometer (Bruker Avance 400) was used for all NMR experiments. A solvent mixture of $CD_2Cl_2$, $CHF_2Cl$, and $CF_3Br$ in a ratio of 1:2:2 was used for low-temperature $^{13}C$ NMR measurements. The temperature of the probe was calibrated by means of a type K (Chromel/Alumel) thermocouple inserted into a dummy tube. The readings are estimated to be accurate within ±2 K. The NMR spectra were loaded into the data-handling program IGOR (WaveMetrics) for analysis, manipulations, and graphic display. Line shape simulations of the NMR spectra were performed by using the WinDNMR program [38].

### 5.4. Computational studies

Calculations for direct comparison and use with the GED experiment were carried out at the M06-2X/aug-cc-pVTZ level of theory (see Table 1) using Gaussian 09 program [68]. NBO analyses of the SCF wave function [42,69–71] and calculations of the total steric energy [39–41] were performed using the NBO 6.0 program [72,73] at the M06-2X/6-311++G** level of theory.

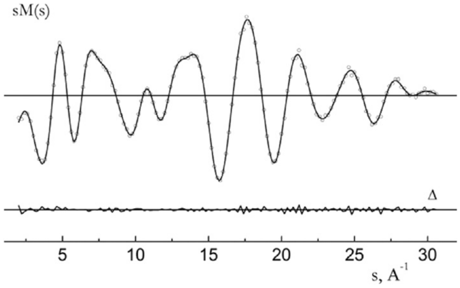

**Fig. 7.** Experimental (dots) and calculated (solid line) combined molecular intensity curves for 1-cyano-1-silacyclohexane as obtained by gas electron diffraction. Below: difference curve (experiment − model).

High-level coupled cluster calculations were carried out (using the ORCA package, version 3.0.3) [74] on MP2/def2-TZVP [75,76] optimized geometries in order to get accurate potential energy differences between the axial and equatorial conformers as shown in Table 5.

Electronic energy differences were calculated using explicitly correlated MP2 and coupled cluster theory [43] as implemented in ORCA. CCSD(T)-F12/CBS (CBS = complete basis set) level energies were estimated by performing large basis MP2-F12 that converge quickly to the complete basis set limit (CBS) and then applying a CCSD(T)-F12 correction to the MP2-F12/large basis value:

$$\Delta E^{\mathrm{CCSD(T)-F12/CBS}} \approx \Delta E^{\mathrm{MP2-F12/large\ basis}} + \left( \Delta E^{\mathrm{CCSD(T)-F12/small\ basis}} - \Delta E^{\mathrm{MP2-F12/small\ basis}} \right)$$

The MP2 calculations were performed with the correlation consistent basis sets for explicitly correlated methods [74] up to the cc-pVQZ-F12 level. The $\Delta E$ value changed by ~0.009 kcal mol$^{-1}$ when going from the TZ-F12 to QZ-F12 for both **2** and **4** compounds and can be considered converged with respect to basis set size. The ($\Delta E^{\mathrm{CCSD(T)-F12/small\ basis}} - \Delta E^{\mathrm{MP2-F12/small\ basis}}$) term was calculated at the CCSD(T)-F12/cc-pVDZ-F12 and MP2/cc-pVDZ-F12 level and was 0.39 kcal mol$^{-1}$ for **2** and 0.24 kcal mol$^{-1}$ for **4**, demonstrating that MP2 calculations can differ considerably from CCSD(T). Auxiliary basis sets (CABS) in the form of cc-pVnZ-F12/OptRI were used in all calculations [76]. Similar CCSD(T)/CBS protocols have been used in studies on silacyclohexanes [14,16].

The enthalpy and entropy corrections to the conformational energies were calculated from harmonic vibrational frequencies at the B3LYP/def2-TZVPP [75] level using ORCA but using the quasi-RRHO approximation [77] by Grimme for low frequencies as implemented in ORCA. Six-membered rings include a number of low-frequency vibrations that are known to be badly predicted by the harmonic approximation and as they contribute significantly to entropy, errors in the entropy correction are to be expected from the regular harmonic approximation. The quasi-RRHO approximation attempts to correct for such errors by replacing the vibrational entropy contribution by a rotational contribution for the low frequencies (below 100 cm$^{-1}$).

Chemical shift calculations were performed using the gauge-independent atomic orbital (GIAO) method [78] using NWChem 6.6, on the MP2 geometries at the PBE0 level of theory and using the aug-pcS-2 basis set on carbon atoms and def2-TZVP on other atoms. Tetramethylsilane was used as a computational reference for converting calculated shieldings into chemical shifts.

## Acknowledgments

A.V.B. and Yu.F.S. are grateful to the Ministry of Education and Science of Russia (State Contracts № 14.B25.31.0013) for financial support. S.A.Sh. thanks the Russian Foundation for Basic Research (Grant 14-03-0023-a). I.A., S.O.W., and N.R.J. thank the Icelandic Centre for Research (RANNIS) for financial support, Grants No 080038021 and 100040022. R.B. acknowledges support from the Icelandic Research Fund, grant no. 141218051.

## Appendix A. Supplementary data

Supplementary data related to this article can be found at http://dx.doi.org/10.1016/j.molstruc.2016.10.012.

## References

[1] E.L. Eliel, S.H. Wilen, Stereochemistry of Organic Compounds, Wiley, New York, 1994.
[2] E. Juaristi, Conformational Behavior of Six-membered Rings, Methods in Stereochemical Analysis, VCH Publishers, Inc., New York, 1995.
[3] I. Arnason, Á. Kvaran, A. Bodi, Int. J. Quantum Chem. 106 (2006) 1975–1978.
[4] S. Winstein, N.J. Holness, J. Am. Chem. Soc. 77 (1955) 5562.
[5] H. Booth, J.R. Everett, J. Chem. Soc. Perkin Trans. II (1980) 255–259.
[6] C.H. Bushweller, in: E. Juaristi (Ed.), Conformational Behavior of Six-membered Rings, VCH Publishers, Inc., New York, 1995, pp. 25–58.
[7] M. Manharan, E.L. Eliel, Tetrahedron Lett. 25 (1984) 3267–3268.
[8] K.B. Wiberg, J.D. Hammer, H. Castejon, W.F. Bailey, E.L. DeLeon, R.M. Jarret, J. Org. Chem. 64 (1999) 2085–2095.
[9] F. Taddei, E. Kleinpeter, J. Mol. Struct. (THEOCHEM) 683 (2004) 29–41.
[10] F. Taddei, E. Kleinpeter, J. Mol. Struct. (THEOCHEM) 718 (2005) 141–151.
[11] F. Cortés-Guzmán, J. Hernández-Trujillo, G. Cuevas, J. Phys. Chem. A 107 (2003) 9253–9256.
[12] I. Arnason, Á. Kvaran, S. Jonsdottir, P.I. Gudnason, H. Oberhammer, J. Org. Chem. 67 (2002) 3827–3831.
[13] L.B. Favero, B. Velino, W. Caminati, I. Arnason, Á. Kvaran, Organometallics 25 (2006) 3813–3816.
[14] T. Kern, M. Hölbling, A. Dzambaski, M. Flock, K. Hassler, S.Ó. Wallevik, I. Arnason, R. Bjornsson, J. Raman Spectrosc. 43 (2012) 1337–1342.
[15] B.A. Shainyan, E. Kleinpeter, Tetrahedron 68 (2012) 114–125.
[16] A.V. Belyakov, Y.F. Sigolaev, S.A. Shlykov, S.Ó. Wallevik, N.R. Jonsdottir, R. Bjornsson, S. Jonsdottir, Á. Kvaran, T. Kern, K. Hassler, I. Arnason, Struct. Chem. 26 (2015) 445–453.
[17] E.L. Eliel, M. Manoharan, J. Org. Chem. 46 (1981) 1959–1962.
[18] M.E. Squillacote, J.M. Neth, J. Am. Chem. Soc. 109 (1987) 198–202.
[19] G.V. Girichev, N.I. Giricheva, A. Bodi, P.I. Gudnason, S. Jonsdottir, Á. Kvaran, I. Arnason, H. Oberhammer, Chem. Eur. J. 13 (2007) 1776–1783.
[20] G.V. Girichev, N.I. Giricheva, A. Bodi, P.I. Gudnason, S. Jonsdottir, Á. Kvaran, I. Arnason, H. Oberhammer, Chem. Eur. J. 15 (2009) 8929.
[21] S.Ó. Wallevik, R. Bjornsson, Á. Kvaran, S. Jonsdottir, I. Arnason, A.V. Belyakov, A.A. Baskakov, K. Hassler, H. Oberhammer, J. Phys. Chem. A 114 (2010) 2127–2135.
[22] J.R. Durig, A.M. El Defrawy, R.M. Ward, G.A. Guirgis, T.K. Gounev, Struct. Chem. 19 (2008) 579–594.
[23] S.Ó. Wallevik, R. Bjornsson, Á. Kvaran, S. Jonsdottir, I. Arnason, A.V. Belyakov, T. Kern, K. Hassler, Organometallics 32 (2013) 6996–7005.
[24] B. Douglas, D. McDaniel, J. Alexander, Concepts and Models of Inorganic Chemistry, John Wiley & Sons, Inc., New York, 1994.
[25] N.L. Allinger, W. Szkrybalo, J. Org. Chem. 27 (1962) 4601–4603.
[26] D. Höfner, S.A. Lesko, G. Binsch, Org. Magn. Reson. 11 (1978) 179–196.
[27] F.R. Jensen, C.H. Bushweller, B.H. Beck, J. Am. Chem. Soc. 91 (1969) 344–351.
[28] D.J. Raber, J. Milton, D. Johnston, M.A. Schwalke, J. Am. Chem. Soc. 99 (1977) 7671–7673.
[29] H.-J. Schneider, V. Hoppen, J. Org. Chem. 43 (1978) 3866–3873.
[30] M. Tichy, F. Sipos, J. Sicher, Collect. Czech. Chem. Commun. 31 (1966) 2889.
[31] J.R. Durig, R.M. Ward, A.R. Conrad, M.J. Tubergen, K.G. Nelson, P. Groner, T.K. Gounev, J. Mol. Struct. 967 (2010) 99–111.
[32] B.A. Shainyan, E. Kleinpeter, Tetrahedron 69 (2013) 5927–5936.
[33] Y. Zhao, D.G. Truhlar, Theor. Chem. Acc. 120 (2008) 215–241.
[34] A.E. Aliev, K.D.M. Harris, J. Am. Chem. Soc. 115 (1993) 6369–6377.
[35] H. Booth, J.R. Everett, R.A. Fleming, Org. Magn. Reson. 12 (1979) 63–66.
[36] H.-O. Kalinowski, S. Berger, S. Braun, 13C-NMR-Spektroskopie, Georg Thieme Verlag, Stuttgart/New York, 1984.
[37] K. Pihlaja, E. Kleinpeter, Carbon-13 NMR Chemical Shifts in Structural and Stereochemical Analysis, VCH Publishers, Inc, New York, 1994.
[38] H.D. Reich, WinDNMR: dynamic NMR spectra for windows, J. Chem. Educ. (1995). Software 3D2.
[39] J.K. Badenhoop, F. Weinhold, J. Chem. Phys. 107 (1997) 5406.
[40] J.K. Badenhoop, F. Weinhold, J. Chem. Phys. 107 (1997) 5422.
[41] J.K. Badenhoop, F. Weinhold, Int. J. Quantum Chem. 72 (1999) 269.
[42] F. Weinhold, Discovering Chemistry with Natural Bond Orbitals, Wiley, Hoboken, New Jersey, 2012.
[43] L. Kong, F.A. Bischoff, E.F. Valeev, Chem. Rev. 112 (2012) 75–107.
[44] A. Klamt, G. Schüürmann, J. Chem. Soc. Perkin Trans. 2 (1993) 799.
[45] A.V. Marenich, C.J. Cramer, D.C. Truhlar, J. Phys. Chem. B 113 (2009) 6378–6396.
[46] A.D. Becke, Phys. Rev. B 38 (1988) 3098–3100.
[47] A.D. Becke, J. Chem. Phys. 98 (1993) 5648.
[48] C. Lee, W. Yang, R.G. Parr, Phys. Rev. B 37 (1988) 785.
[49] P.J. Stephens, F.J. Devlin, C.F. Chabalowski, M.J. Frisch, J. Phys. Chem. 98 (1994) 11623–11627.
[50] S. Grimme, J. Antony, S. Ehrlich, H. Krieg, J. Phys.Chem. 132 (2010) 154104.
[51] S. Grimme, S. Ehrlich, L. Goerigk, J. Comput. Chem. 32 (2011) 1456–1465.
[52] F. Weigend, R. Ahlrichs, Phys. Chem. Chem. Phys. 7 (2005) 3297–3305.
[53] A. Bodi, Á. Kvaran, S. Jonsdottir, E. Antonsson, S.Ó. Wallevik, I. Arnason, A.V. Belyakov, A.A. Baskakov, M. Hölbling, H. Oberhammer, Organometallics 26 (2007) 6544–6550.
[54] L.B. Favero, B. Velino, W. Caminati, I. Arnason, Á. Kvaran, J. Phys. Chem. A 110 (2006) 9995–9999.
[55] A.V. Belyakov, A.A. Baskakov, R.J.F. Berger, N.W. Mitzel, H. Oberhammer, I. Arnason, S.Ó. Wallevik, J. Mol. Struct. 1012 (2012) 126–130.
[56] B.A. Shainyan, S.V. Kirpichenko, D.Y. Osadchiy, S.A. Shlykov, Struct. Chem. 25 (2014) 1677–1685.
[57] B.A. Shainyan, S.V. Kirpichenko, E. Kleinpeter, S.A. Shlykov, D.Y. Osadchiy, N.N. Chipanina, L.P. Oznobikhina, J. Org. Chem. 78 (2013) 3939–3947.
[58] B.A. Shainyan, S.V. Kirichenko, N.N. Chipanina, L.P. Oznobikhina, E. Kleinpeter, S.A. Shlykov, D.Y. Osadchiy, J. Org. Chem. 80 (2015) 12492–12500.
[59] S.V. Kirpichenko, E. Kleinpeter, I.A. Ushakov, B.A. Shainyan, J. Phys. Org. Chem. 24 (2013) 320–326.
[60] S.A. Shlykov, D. Osadchiy, N.N. Chipanina, L.P. Oznobikina, B.A. Shainyan, J. Mol. Struct. 1100 (2015) 555–561.
[61] G.V. Girichev, S.A. Shlykov, V.N. Petrova, N.Y. Subbotina, S.B. Lapshina, T.G. Danilova, Izv Vyssh Uchebn Zaved Khim Khim Tekhnol. 31 (1988) 46 (in Russian).
[62] G.V. Girichev, S.A. Shlykov, Y.F. Revichev, Instrum. Exp. Tech. (Engl. Transl.) 2 (1984) 457, 4 (1986) 167.
[63] G.V. Girichev, A.N. Utkin, Y.F. Revichev, Instrum. Exp. Tech. (Engl. Transl.) 2 (1984) 457. N2 (1984) 187.
[64] E.G. Girichev, A.V. Zakharov, G.V. Girichev, M.I. Bazanov, Izv. VUZ Tekstiln. Prom. 2 (2000) 142 (Russian).
[65] A.W. Ross, M. Fink, R.L. Hilderbrandt, International Tables of Crystallography, C, Kluwer Acad. Publ., Dordrecht, 1992, p. 245.
[66] B. Andersen, H.M. Seip, T.G. Strand, R. Stolevik, Acta Chem. Scand. 23 (1969) 3224.
[67] G. Gundersen, S. Samdal, H.M. Seip, Least Squares Structural Refinement Program Based on Gas Electron-diffraction Data, vols. I–III, Department of Chemistry, University of Oslo, Oslo, 1981, p. 116.
[68] M.J. Frisch, G.W. Trucks, H.B. Schlegel, G.E. Scuseria, M.A. Robb, J.R. Cheeseman, G. Scalmani, V. Barone, B. Mennucci, G.A. Petersson, H. Nakatsuji, M. Caricato, X. Li, H.P. Hratchian, A.F. Izmaylov, J. Bloino, G. Zheng, J.L. Sonnenberg, M. Hada, M. Ehara, K. Toyota, R. Fukuda, J. Hasegawa, M. Ishida, T. Nakajima, Y. Honda, O. Kitao, H. Nakai, T. Vreven, J.A. Montgomery Jr., J.E. Peralta, F. Ogliaro, M. Bearpark, J.J. Heyd, E. Brothers, K.N. Kudin, V.N. Staroverov, R. Kobayashi, J. Normand, K. Raghavachari, A. Rendell, J.C. Burant, S.S. Iyengar, J. Tomasi, M. Rega Cossi, N.J. Millam, M. Klene, J.E. Knox, J.B. Cross, V. Bakken, C. Adamo, J. Jaramillo, R.E. Gomperts, O. Stratmann, A.J. Yazyev, R. Austin, C. Cammi, J.W. Pomelli, R. Ochterski, R.L. Martin, K. Morokuma, V.G. Zakrzewski, G.A. Voth, P. Salvador, J.J. Dannenberg, S. Dapprich, A.D. Daniels, O. Farkas, J.B. Foresman, J.V. Ortiz, J. Cioslowski, D. Fox, Gaussian 09, Revision D01, Gaussian, Inc., Wallingford CT, 2009.
[69] Encyclopedia of Computational Chemistry 1998-11, vols. 1–5, John Wiley & Son, Chechester, NY, 1998.
[70] E.D. Glendening, C.R. Landis, F. Weinhold, WIREs Comput. Mol. Sci. 2 (2012) 1–42.
[71] F. Weinhold, C.R. Landis, Valency and Bonding: a Natural Bond Orbital Donor-acceptor Perspective, Cambridge University Press, Cambridge, 2005, p. p 760.
[72] E.D. Glendening, J.K. Badenhoop, A.E. Reed, J.E. Carpenter, J.A. Bohmann, C.M. Morales, C.R. Landis, F. Weinhold, Natural Bond Orbital Analysis Program: NBO 6.0, Theoretical Chemistry Institute, University of Wisconsin, Madison, WI, 2013.
[73] E.D. Glendening, C.R. Landis, F. Weinhold, J. Comput. Chem. 34 (2013) 1429–1437.
[74] K.A. Peterson, T.B. Adler, H.J. Werner, J. Chem. Phys. 128 (2008) 084102.
[75] F. Weigend, R. Ahlrichs, Phys. Chem. Chem. Phys. 7 (2005) 3297.
[76] K.E. Yousaf, K.A. Peterson, J. Chem. Phys. 129 (2008) 184108.
[77] S. Grimme, Chem. Eur. J. 18 (2012) 9955–9964.
[78] R. Dichtfield, Mol. Phys. 27 (1974) 789–807.